

Contribution to Case C1.1: Inviscid Flow through a Channel with a Smooth Bump

Original

Contribution to Case C1.1: Inviscid Flow through a Channel with a Smooth Bump / Ferrero, A.; Larocca, F.. - ELETTRONICO. - (2013). (Intervento presentato al convegno 2nd International Workshop on High-Order CFD Methods tenutosi a Cologne, Germany nel 27--28 May 2013).

Availability:

This version is available at: 11583/2701814 since: 2018-02-27T10:30:46Z

Publisher:

Published

DOI:

Terms of use:

openAccess

This article is made available under terms and conditions as specified in the corresponding bibliographic description in the repository

Publisher copyright

(Article begins on next page)

2nd International Workshop on High-Order CFD Methods
May 27-28, 2013, Cologne, Germany

Abstract available at:
http://www.dlr.de/as/desktopdefault.aspx/tabid-8170/13999_read-39370/

Case C1.2: Inviscid Flow through a Channel with a Smooth Bump

Andrea Ferrero* and Francesco Larocca[†]

*Department of Mechanical and Aerospace Engineering
Politecnico di Torino, Italy*

1 Code description

Numerical simulations were performed with an high-order discontinuous Galerkin code written in Fortran 90 which can solve Euler equations. Several approximate Riemann problem solvers are available for the computation of convective fluxes. In particular all simulations were performed with the Osher solver. The numerical solution inside the element is represented with a modal basis obtained by a tensor product of Legendre polynomials. Integrals are approximated by Gauss quadrature formulas. Discontinuities can be stabilized with both limiters or adaptive filters. Curvilinear boundaries can be represented with quadrilateral elements transformed with high-order Serendipity mapping (linear, parabolic, cubic and quartic curvilinear elements are available). Time integration is performed with explicit Runge Kutta algorithms up to 4th order. Parallelization is supported on shared memory machines with OpenMP directives.

2 Case summary

2.1 Boundary conditions and mesh

Subsonic characteristic inflow and outflow boundary conditions are imposed at the inlet and at the outlet. Lateral boundaries are represented as inviscid solid walls. Tangency is imposed by the solution of a particular Riemann problem in which the wall state is forced to have zero normal velocity.

Simulations were performed on three structured meshes with 16x4, 32x8, 64x16 and 128x32 quadrilateral elements. The edges of the elements on the bottom wall are curved by the introduction of additional points. In particular we use second, third and fourth order Serendipity mapping for wall elements with $p=1$, $p=2$ and $p=3$ discretizations. Elements which are not in contact with the wall are always mapped with the classical bilinear mapping.

*PhD candidate, email: andrea.ferrero@polito.it

[†]Professor, email: francesco.larocca@polito.it

2.2 Error computation

The L_2 norm of the entropy is evaluated according to the following expression

$$L_2 s = \sqrt{\frac{\sum_e \int_{\Omega_e} (\Delta s)^2 dV}{\int_{\Omega} dV}} = \sqrt{\frac{\sum_e \sum_i \sum_j (\Delta s)^2 |J| w_i w_j}{\sum_e \sum_j \sum_j |J| W_i W_j}} \quad (1)$$

$$\Delta s = \frac{\frac{p}{\rho^\gamma} - \frac{p_\infty}{\rho_\infty^\gamma}}{\frac{p_\infty}{\rho_\infty^\gamma}} \quad (2)$$

in which Δs , $|J|$, w_i and w_j represent the entropy error, the Jacobian determinant and the Gauss quadrature weights. In particular we use for this computation the same tensor products of Gauss quadrature formulas used for mass matrix evaluation: 2x2 points for $p=1$, 3x3 points for $p=2$, 4x4 points for $p=3$.

2.3 Time discretization and time step

The code is still under development and at the moment we integrate the solution in time using explicit Runge-Kutta algorithms. For $p=1$ and $p=2$ we use TVD-RK2 and TVD-RK3 algorithm. For $p=3$ we use SSP-RK4 algorithm. The time step is chosen according to the following stability limit ([1]):

$$\Delta t = \frac{\sigma \Delta x}{\lambda(2k+1)} \quad (3)$$

in which λ is the maximum propagation speed for the signals inside the cell, Δx is a representative cell dimension and p is the order of the polynomial reconstruction. In order to accelerate convergence we start the simulation working with the first order in space and time scheme, we reduce the density residual of 5 order of magnitude and then we activate the second order in space and time scheme. We repeat this procedure until we activate the scheme with the desired order of accuracy. Starting from that point we integrate in time until the L_2 -norm of the density residual is dropped by 10 orders of magnitude. In particular we monitor the residual of the zero order density modal coefficient, which represents the average density in the element. Numerical solution is initialized with a uniform $M_\infty = 0.5$ field.

2.4 Hardware specification

All computations were performed on a Linux machine with two Intel64 E5504 processors with 8 cores in total. The machine produces a Taubench time of 13.82 s on a single core. The number of employed cores is from 1 to 8, depending on the mesh size and scheme order.

3 Results

In Fig.1 and 2 we report the entropy L_2 error as a function of the lenght scale and work units for different meshes. Fig. 2 shows clearly the need of multigrid

techniques or implicit integration methods in order to make high order schemes more advantageous respect to low order schemes in steady state problems.

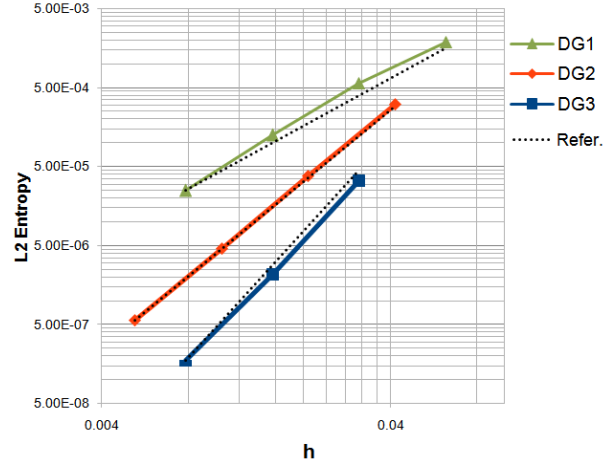


Figure 1: Entropy L2 error vs length scale

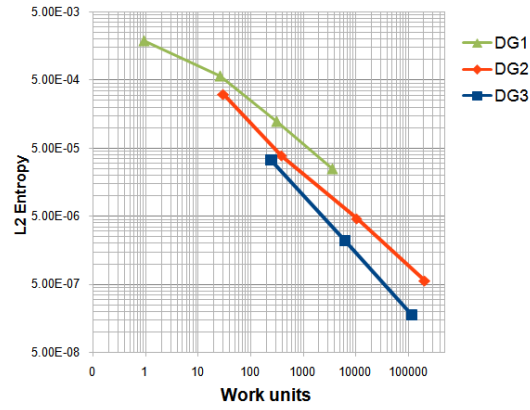


Figure 2: Entropy L2 error vs work units

p	Work units
1	3.9
2	5.5
3	10.7

Table 1: Work Units for 100 residual evaluations with 250000 DOFs

References

- [1] V. Wheatley, H. Kumar, P. Huguenot, On the role of Riemann solvers in Discontinuous Galerkin methods for magnetohydrodynamics, J. Compu. Phys. 229 (2010) 660-680.